Discrete Wavelet Transforms of the Finite Spectrum Digital Images

Viktor P. Dvorkovich
Multimedia Technology and Telecom. Department
Moscow Institute of Physics and Technology
Moscow, Russian Federation
dvp@niircom.ru

Alexander V. Dvorkovich
Multimedia Systems and Technology Lab.
Moscow Institute of Physics and Technology
Moscow, Russian Federation
a_dvork@niircom.ru

Abstract—**A new approach for calculation of wavelet basis for multiscale wavelet decomposition of digital images is proposed. Two, three, four and five sub-band filter banks for decomposition and restoration of images are presented.**

Keywords-multiscale analysis, wavelet decomposition, FIR filters, sub-band image coding

I. INTRODUCTION

The concept of digital image multiscale analysis with finite spatial spectrum consists in a representation of signal waveform as a sequence of approximations from a coarse one to more fines on different slots of base domain [1-3].

Previously two-channel frequency decomposition has been usually implemented in signal coding – low frequency (LF) and high frequency (HF) as shown on the Fig. 1.

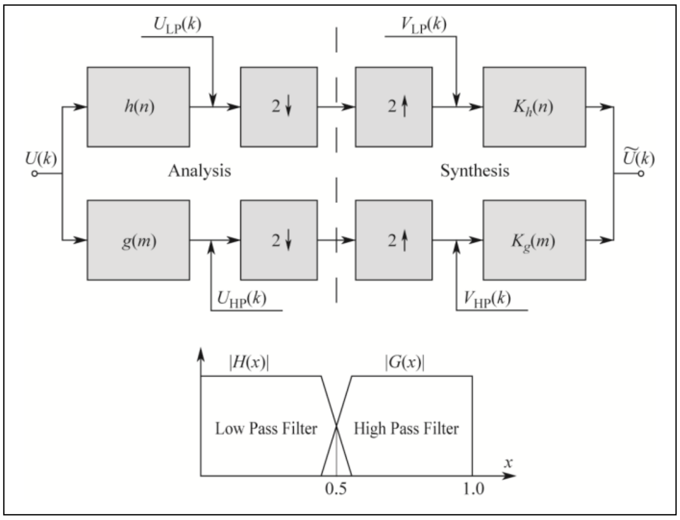

Figure 1. Block diagram of a two-band system of sub-band transform and coding.

II. TWO-BAND FILTER BANK

A new method for calculation of wavelet filter banks useful for image decomposition in presented here. Orthogonal finite impulse response (FIR) filters with either an odd number of tuples and linear (zero) phase frequency response (PFR) (Fig. 2), or with an even number of tuples (Fig. 3) are commonly applied [4].

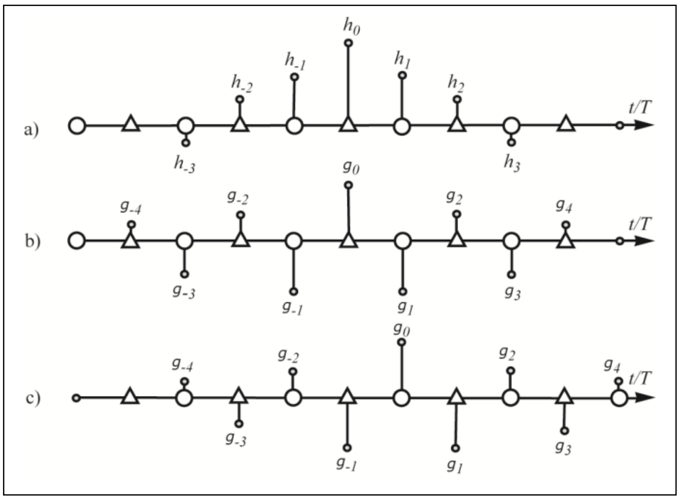

Figure 2. Pulse response of LF (a) and HF (b, c) odd tuple wavelet transform filters.

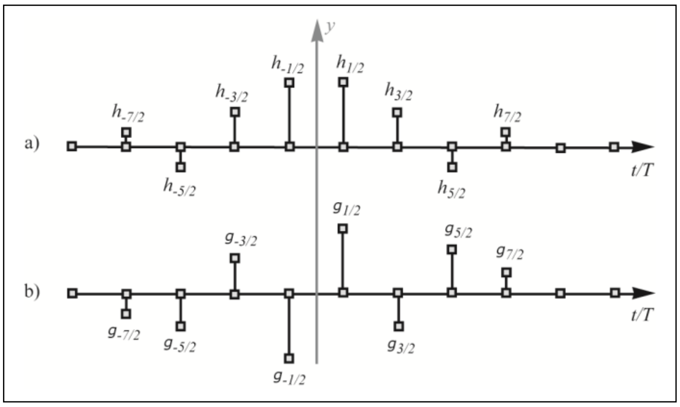

Figure 3. Pulse response of LF (a) and HF (b) even tuple wavelet transform filters.

In the first case if LF and HF wavelet filters may be represented as follows:

This work was supported by Russian Ministry of Education and Science under Grant ID RFMEFI58115X0015.

$$\begin{aligned} H(x) &= h_0 + 2\sum_{n=1}^{N} h_n \cos(\pi n x), \\ G(x) &= g_0 + 2\sum_{m=1}^{M} g_m \cos(\pi m x), \\ \bar{H}(x) &= h_0 + 2\sum_{n=1}^{N} (-1)^n h_n \cos(\pi n x), \\ \bar{G}(x) &= g_0 + 2\sum_{m=1}^{M} (-1)^m g_m \cos(\pi m x), \end{aligned} \quad 0 \le x \le 1 \qquad (1)$$

and the reverse filter forms may be derived as:

$$\begin{cases} \bar{H}(z)\cdot Kh(z) \pm \bar{G}(z)\cdot Kg(z) = 0, \\ H(z)\cdot Kh(z) + G(z)\cdot Kg(z) = 2, \end{cases} \qquad (2)$$

where using of the minus sign corresponds to co-phase placement of LF and HF filter tuples as in Fig. 2 (a, b) and using the plus sign corresponds to shifted placement of LF and HF filter tuples as in Fig. 2 (a, c).

The determinant of the equation system equals to the following constant:

$$A_0 = 2\left(h_0 g_0 + 2\sum_{n=1}^{\min\{N,M\}} (-1)^n h_n g_n \right) \qquad (3)$$

and in this case

$$\begin{cases} H(0) = h_0 + 2\sum_{n=1}^{N} h_n = \sqrt{2}, \\ H(1) = h_0 + 2\sum_{n=1}^{N} (-1)^n h_n = 0, \\ G(0) = g_0 + 2\sum_{n=1}^{M} g_m = 0, \\ G(1) = g_0 + 2\sum_{n=1}^{M} (-1)^m g_m = \sqrt{2}. \end{cases} \qquad (4)$$

Accounting for the need for $N + M + 2$ equations to solve the system by parameters h_n, $0 \le n \le N$, and g_m, $0 \le m \le N$, it is worth to equate to zero the even moments of functions $H(x)$ and $G(x)$ – $H^{(2r)}(x)\big|_{x=0 \text{ or } x=1}$, $r = 1, 2, 3, \dots$ and $G^{(2p)}(x)\big|_{x=0 \text{ or } x=1}$, $p = 1, 2, 3, \dots$

Amplitude frequency responses (AFR) of some filters calculated according to the algorithm described above are illustrated on Fig. 4. These filters are identical to the filters used in JPEG2000 standard [5, 6].

In the second case (Fig. 3) frequency characteristics of respective filters may be obtained as:

$$\begin{aligned} H(x) &= 2\sum_{n=1}^{N} h_{(2n-1)/2} \cos(\pi \frac{2n-1}{2} x), \\ G(x) &= -2j\sum_{m=1}^{M} g_{(2n-1)/2} \sin(\pi \frac{2m-1}{2} x). \end{aligned} \qquad (5)$$

And the filter calculation defined as:

$$\begin{cases} \bar{H}(x)\cdot Kh(x) + \bar{G}(x)\cdot Kg(x) = 0, \\ H(x)\cdot Kh(x) + G(x)\cdot Kg(x) = 2, \end{cases} \qquad (6)$$

where $\bar{H}(x) = 2j\sum_{n=1}^{N} (-1)^n h_{(2n-1)/2} \sin(\pi \frac{2n-1}{2} x)$, $\bar{G}(x) = -2\sum_{m=1}^{M} (-1)^n g_{(2m-1)/2} \cos(\pi \frac{2m-1}{2} x)$, $Kh(x) = \bar{G}(x)$, $Kg(x) = \bar{H}(x)$.

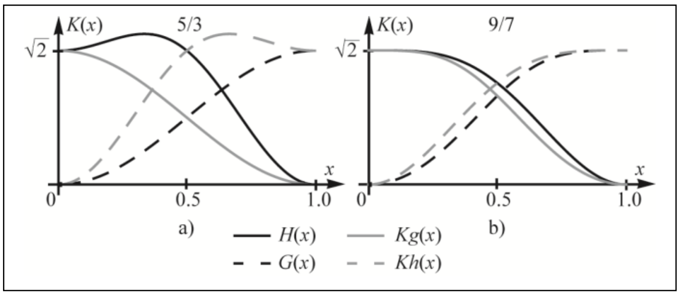

Figure 4. AFR of analysis and synthesis wavelet filters 5/3 (a) and 9/7 (b).

AFR of some filters calculated according to the second algorithm are illustrated on Fig. 5.

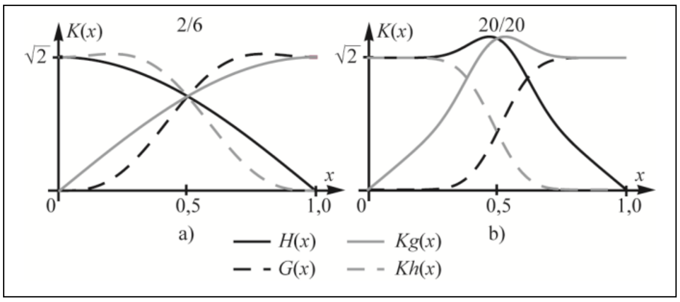

Figure 5. AFR of analysis and synthesis wavelet filters 2/6 (a) and 20/20 (b).

III. THREE-, FOUR- AND FIVE-BAND FILTER BANKS

The approach presented above may be used for calculation of multiple-band wavelet filters banks.

On the Fig. 6 a block diagram of a three-channel system of sub-band coding and decoding is shown, and Fig. 7 presents pulse responses of LF (a), MF (middle frequency) (b) and HF (c) filters.

LF, MF and HF wavelet filters may be represented as follows:

$$H(x) = h_0 + 2\sum_{n=1}^{N} h_n \cos(\pi n x),$$
$$B(x) = 2j\sum_{m=1}^{M} b_m \sin(\pi m x), \qquad (7)$$
$$G(x) = g_0 + 2\sum_{k=1}^{K} g_k \cos(\pi k x).$$

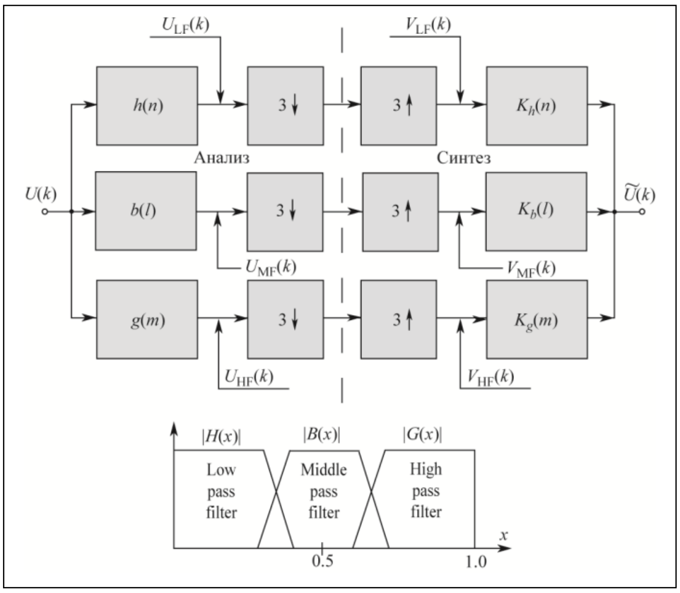

Figure 6. Block diagram of a three-band system.

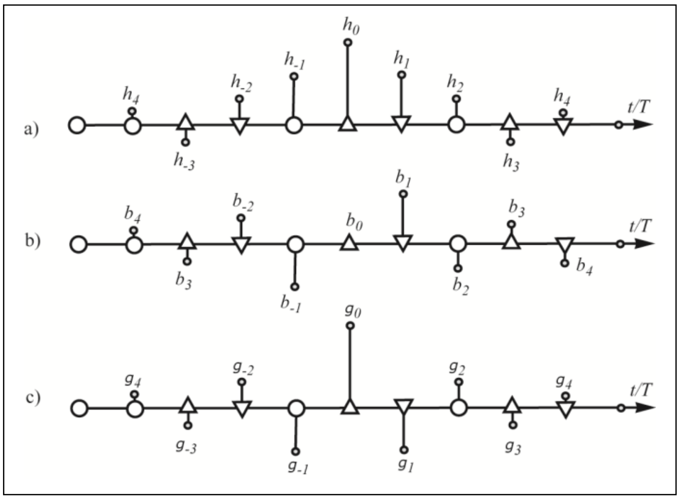

Figure 7. Pulse response of LF (a), MF (b) and HF (c) wavelet transform filters.

Reverse filters are calculated as follows:

$$\begin{cases} H_{\mathrm{O}}(x)Kh(x) + B_{\mathrm{O}}(x)Kb(x) + G_{\mathrm{O}}(x)Kg(x) = 1, \\ H_{\nabla}(x)Kh(x) + B_{\nabla}(x)Kb(x) + G_{\nabla}(z)Kg(z) = 1, \\ H_{\Delta}(x)Kh(x) + B_{\Delta}(x)Kb(x) + G_{\Delta}(z)Kg(z) = 1. \end{cases} \qquad (8)$$

Fig. 8 shows some examples of three-band filter characteristics.

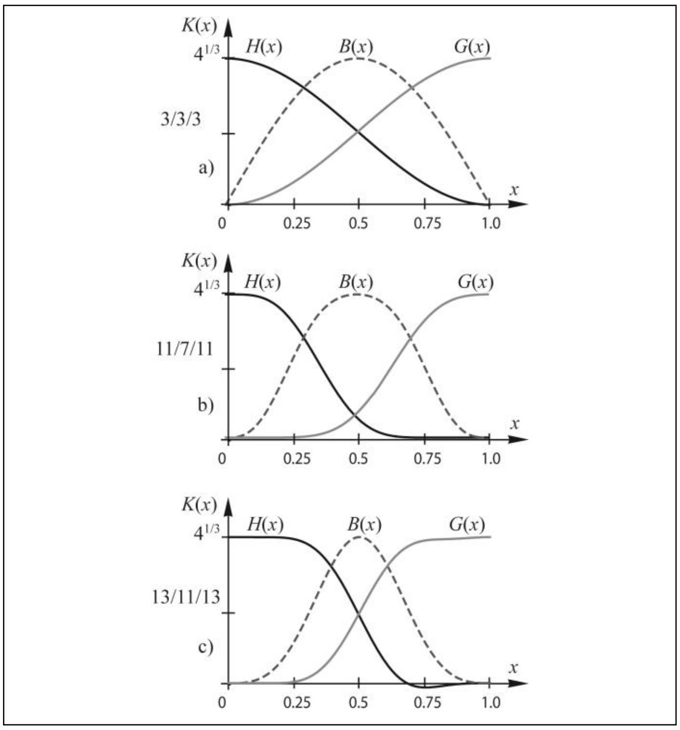

Figure 8. AFR of three-band analysis wavelet filters 3/3/3 (a), 11/7/11 (b) and 13/11/13 (c).

On the Fig. 9 a block diagram of a four-band system of sub-band coding and decoding is shown, and Fig. 10 depicts the pulse response of LF pass filter (a), lower middle frequency (LMF) pass filter (b), higher middle frequency (HMF) pass filter (c) and HF pass filter (d).

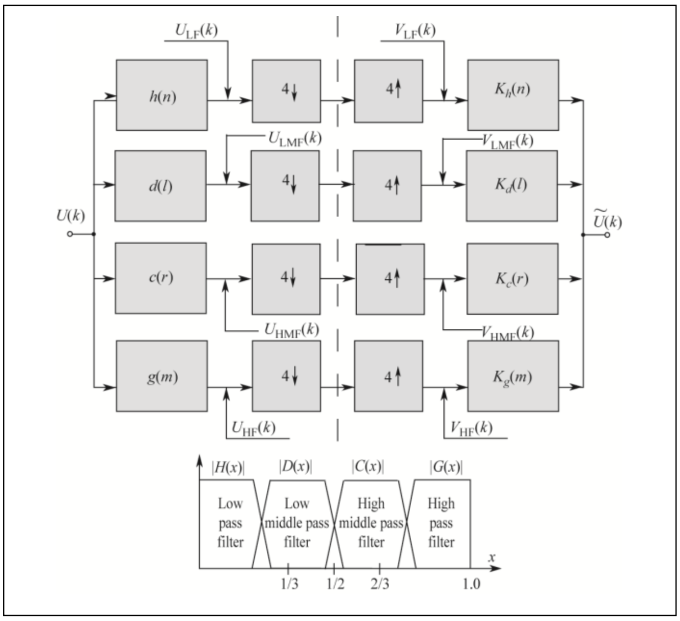

Figure 9. Four sub-band system.

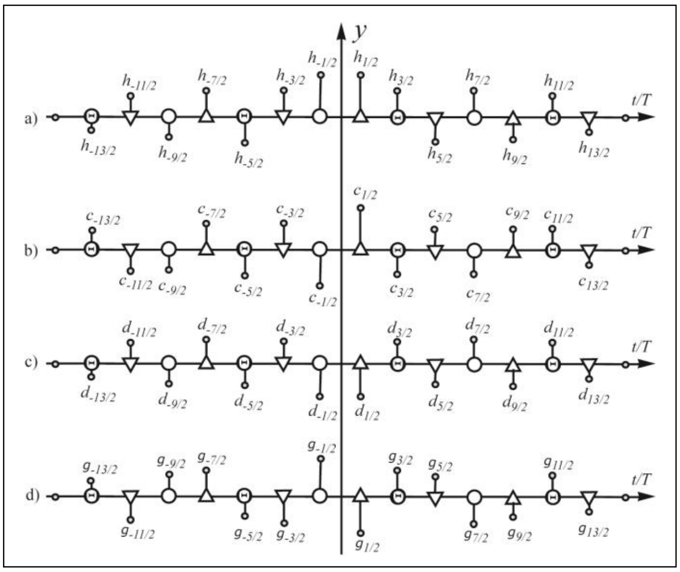

Figure 10. Pulse response of LF (a), LMF (b), HMF (c) and HF (d) wavelet transform filters.

Here we have:

$$
\begin{aligned}
H(x) &= 2\sum_{n=1}^{N} h_{n-1/2}\cos\ \frac{2n-}{2}\pi x\Big), \\
C(x) &= 2\sum_{m=1}^{M} c_{m-1/2}\cos\Big(\frac{2m-}{2}\pi x\Big), \\
D(x) &= 2\sum_{l=1}^{L} d_{l-1/2}\sin\ \frac{2l-}{2}\pi x\Big), \\
G(x) &= 2\sum_{k=1}^{K} g_{k-1/2}\sin\Big(\frac{2k-}{2}\pi x\Big).
\end{aligned}
\tag{9}
$$

Calculation of the reverse wavelet filter system characteristics is performed using the following system:

$$
\begin{cases}
H_{\mathrm{O}}(x)Kh(x)+D_{\mathrm{O}}(x)Kd(x) \\
\quad C_{\mathrm{O}}(x)Kc(x)+G_{\mathrm{O}}(x)Kg(x)\quad 1, \\
H_{\nabla}(x)Kh(x)\quad D_{\nabla}(x)Kd(x)+ \\
\quad C_{\nabla}(x)Kc(x)\quad G_{\nabla}(z)Kg(z)=1, \\
H_{\Delta}(x)Kh(x)\quad D_{\Delta}(x)Kd(x)+ \\
\quad C_{\Delta}(x)Kc(x)\quad G_{\Delta}(z)Kg(z)=1, \\
H_{\Theta}(x)Kh(x)+D_{\Theta}(x)Kd(x) \\
\quad C_{\Theta}(x)Kc(x)+G_{\Theta}(z)Kg(z)\quad 1.
\end{cases}
\tag{10}
$$

Fig. 11 gives examples of four-band filter characteristics.

A block diagram of a five-band system of sub-band coding and decoding is shown on the Fig. 12. Fig. 13 illustrates the pulse response of LF (a), LMF (b), MF (c), HMF (d) and HF (e) pass filters.

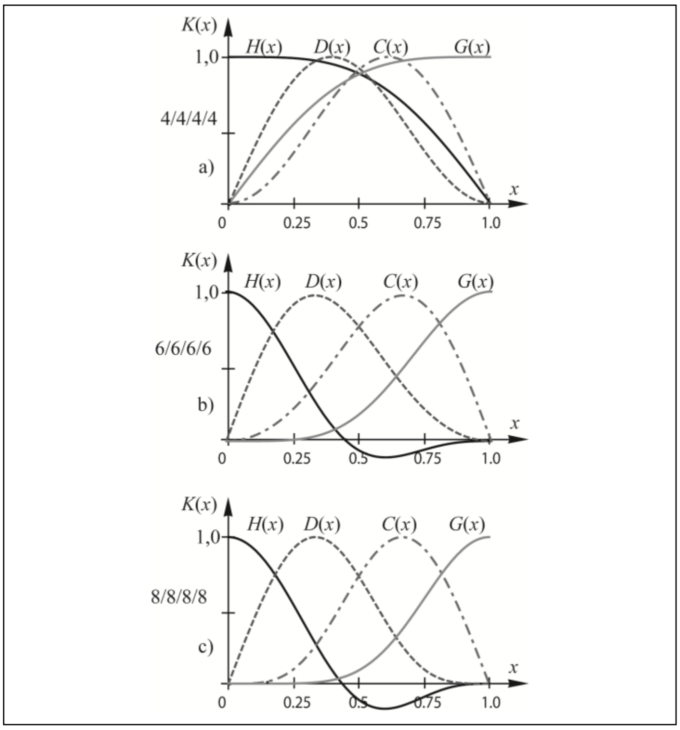

Figure 11. AFR of four-band analysis wavelet filters 4/4/4/4 (a), 6/6/6/6 (b) and 8/8/8/8 (c).

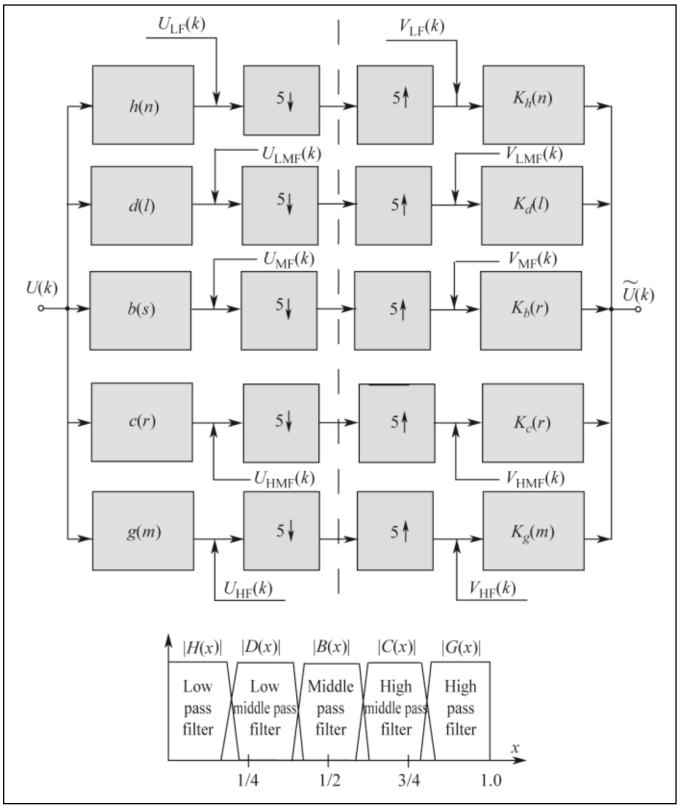

Figure 12. Five sub-band system.

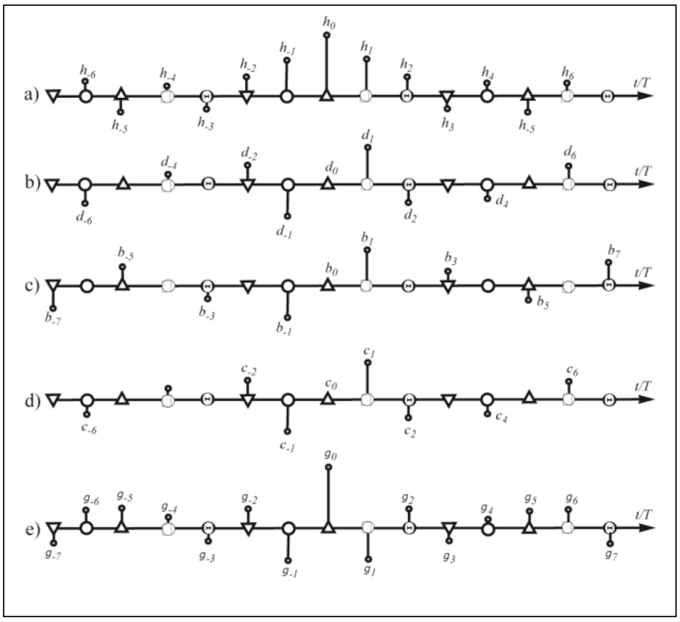

Figure 13. Pulse response of LF (a), LMF (b), MF (c), HMF (d) and HF (e) wavelet transform filters.

In this case we have:

$$
\begin{aligned}
&H(x) = h_0 + 2\sum_{n=1}^{N} h_n \cos(n\pi x),\\
&D(x) = 2j\sum_{l=1}^{L} d_l \sin(l\pi x), \quad d_0 \equiv 0,\\
&B(x) = 2j\sum_{r=1}^{R} b_r \sin(r\pi x), \quad b_0 \quad 0, \quad \text{or}\\
&\quad B(x) = b_0 + 2\sum_{r=1}^{R} b_r \cos(r\pi x),\\
&C(x) = 2j\sum_{m=1}^{M} c_m \sin(m\pi x), \quad c_0 \quad 0,\\
&G(x) = g_0 + 2\sum_{k=1}^{K} g_k \cos(k\pi x).
\end{aligned}
\tag{11}
$$

Calculation of the reverse wavelet filter system characteristics is performed using the following system:

$$
\begin{cases}
H_{\text{O}}(x)Kh(x) + D_{\text{O}}(x)Kd(x) + B_{\text{O}}(x)Kb(x) + \\ \quad C \ \ (x)Kc(x) \quad G_{\text{O}}(x)Kg(x) = 1,\\
H_{\nabla}(x)Kh(x) + D_{\nabla}(x)Kd(x) + B_{\nabla}(x)Kb(x) + \\ \quad C \ \ (x)Kc(x) \quad G_{\nabla}(z)Kg(z) = 1,\\
H_{\Delta}(x)Kh(x) + D_{\Delta}(x)Kd(x) + B_{\Delta}(x)Kb(x) + \\ \quad C \ \ (x)Kc(x) \quad G_{\Delta}(z)Kg(z) = 1,\\
H_{\Theta}(x)Kh(x) + D_{\Theta}(x)Kd(x) + B_{\Theta}(x)Kb(x) + \\ \quad C \ \ (x)Kc(x) \quad G_{\Theta}(z)Kg(z) = 1,\\
H_{\oplus}(x)Kh(x) + D_{\oplus}(x)Kd(x) + B_{\oplus}(x)Kb(x) + \\ \quad C \ \ (x)Kc(x) \quad G_{\oplus}(z)Kg(z) = 1.
\end{cases}
\tag{12}
$$

Fig. 14 shows some five-band filter characteristics.

Figure 14. AFR of five-band analysis wavelet filters 5/5/3/5/5 (a), 7/5/7/5/7

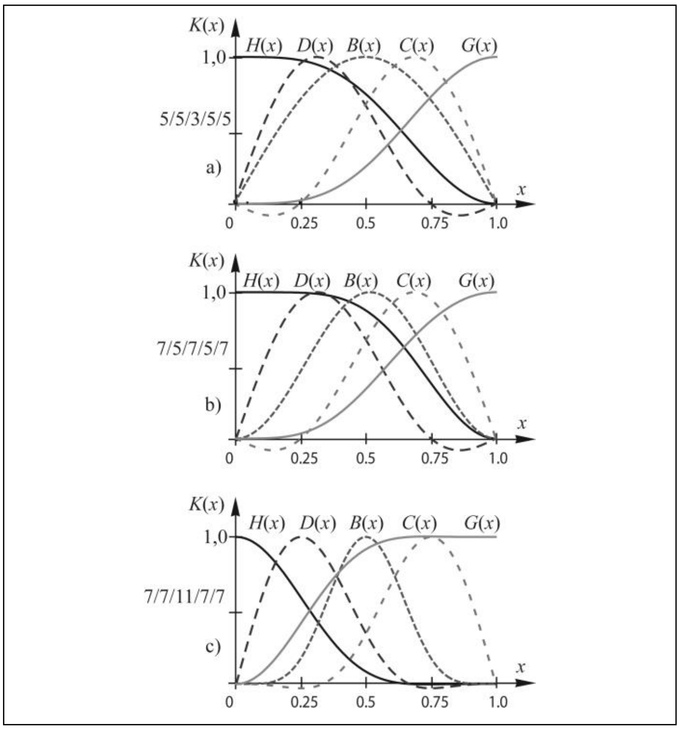

(b) and 7/7/11/7/7 (c).

IV. Conclusion

A new method for multi-band wavelet filter bank calculation was presented. This method allows to create both standard filters (for example, filters used in JPEG2000 standard) and filters with characteristics needed for special purposes, particularly for multi-band wavelet decomposition of images.

References

[1] I. Daubechies, "Ten Lectures on Wavelets", Society for Industrial and Applied Mathematics, Philadelphia, Pennsylvania, 1992.

[2] Ch. Blatter, "Wavelets: A Primer", A K Peters/CRC Press, 1999.

[3] H.-G. Stark, "Wavelets and Signal Processing: An Application-Based Introduction", Springer, 2005.

[4] V.P. Dvorkovich, A.V. Dvorkovich, "Window Functions for Harmonic Analysis of Signals", Moscow: Technosfera, 2014.

[5] ITU-T Recommendation T.800, "Information Technology - JPEG 2000 Image Coding System: Core Coding System", ITU, 2015.

[6] ITU-T Recommendation T.801, "Information Technology - JPEG 2000 Image Coding System: Extensions", ITU, 2002.